Triclinic Fluid Order

Nattaporn Chattham,[1] Eva Korblova,[2,3] Renfan Shao,[2,4] David M. Walba,[2,3] Joseph E. Maclennan,[2,4] and Noel A. Clark[2,4]

[1]*Department of Physics, Faculty of Science, Kasetsart University, Bangkok 10900, Thailand*
[2]*Liquid Crystal Materials Research Center*
[3]*Department of Chemistry and Biochemistry, University of Colorado, Boulder, Colorado 80309, USA*
[4]*Department of Physics, University of Colorado, Boulder, Colorado 80309, USA*

(Received 25 August 2009; published 9 February 2010)

Among the condensed phases, those of lowest point group symmetry are the triclinic crystals, which have only the identity element or the identity and inversion elements. Such low symmetry is stabilized by the specificity of molecular interaction, which is weakened with increasing disorder, so that known phases with fluid degrees of freedom are more symmetric. Here we report triclinic order, appearing as a broken symmetry in a single, isolated, fluid smectic liquid crystal layer freely suspended in air, showing that none of its principal dielectric axes lies either normal or parallel to the layer plane.

DOI: 10.1103/PhysRevLett.104.067801 PACS numbers: 61.30.Eb, 61.30.Gd

In his 1975 monograph [1], de Gennes proposed as a "far-fetched possibility" a tilted smectic phase of fluid layers with biaxial orientational ordering such that none of the principal Cartesian axes of its macroscopic tensor quantities (e.g., the dielectric or diamagnetic susceptibilities) lies either normal or parallel to the layer planes, called the SmCG (G for generalized). The layers of such a phase would have only inversion symmetry and therefore belong to the Schoenflies point symmetry class C_i [2], illustrated in Fig. 1. Here the biaxial optical dielectric tensor of a layer of molecular laths, represented by the red, orange, or yellow box, orients such that none of the faces of the box lies either normal or parallel to the layer plane. If, in addition, the molecules were to have spontaneous *polar* ordering (SmCPG), as is the case, for example, in bent-core molecular systems [3], they would also lack inversion symmetry and thus be chiral, belonging to the class C_1 of the least-symmetric fluids. Among the phases having fluid degrees of freedom in which the symmetry has been directly probed, the smectic liquid crystals (LCs) of polar ordered, tilted bent-core molecules [4], or of tilted chiral rod-shaped molecules [5] have the lowest symmetry. These are monoclinic, of the class C_2, with only a twofold rotation axis, parallel to the layers and normal to the (tilt) plane, as shown in Fig. 1 and verified by detailed optical measurements of their structure [6–8].

In this Letter, we employ smectic LC films, freely suspended in air [9], to isolate and probe single smectic layers in an inherently symmetric environment, enabling a quantitative optical assessment of their ordering. Observations of single-layer films of the bent-core molecular compound NORABOW (Fig. 1) [10] yield unambiguous evidence of a liquid C_1 structure, the "monolayer SmCPG", translationally invariant in the layer plane and exhibiting three broken symmetries: collective polar molecular orientational ordering, and coherent rotation of the molecular plane about two orthogonal Euler axes. Determination of the corresponding Euler angles for tilt of the molecular plane and rotation about the molecular long axis constitute the first measurement of triclinic order parameters in a fluid system. The behavior of NORABOW is contrasted with that of the classic bent-core LC NOBOW (Fig. 1) [11], which maintains its monoclinic C_2 layer structure even in the asymmetric environments of multilayer films. These observations support recent claims of C_1 behavior in bent-core systems in which the layer structure has not been established [12–18].

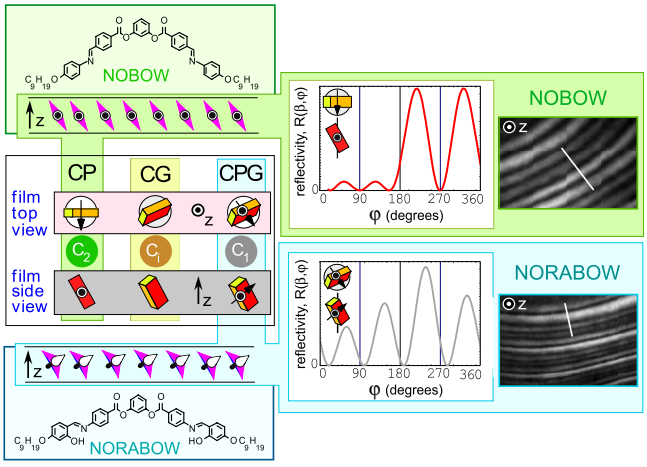

FIG. 1 (color online). Sketches of the monoclinic (C_2) and triclinic (C_i, C_1) orientation states of single smectic layers of the bent-core molecules NOBOW and NORABOW, respectively. Since the molecules exhibit macroscopic polar order due to their bent shape (arrows), the triclinic state is C_1. Their dielectric principal axes are represented by the red, orange, or yellow parallelepipeds, where z is the layer normal. The depolarized layer reflectivity vs long axis tilt azimuth φ, calculated from an optical model of the layer with crossed analyzer ($\beta = 0$), directly reveals the individual layer symmetry. DRLM images show ring winding patterns exhibiting the corresponding optical profiles.

NORABOW, which has the bulk phase sequence: Isotropic (I) (177 °C) SmCPG (99 °C) SmX on cooling, has a structure similar to NOBOW, which exhibits fluid smectic phases with spontaneous polar molecular orientational ordering [3], and monoclinic (C_2) chiral tilt of the molecular plane in fluid smectic B2 phases [4]. In the bulk, the high temperature smectic phase of NORABOW, which we call SmCPG, exhibits the B2-like formation of macroscopically polar and chiral conglomerate domains [10]. X-ray diffraction shows that the NORABOW SmCPG has a simple lamellar fluid structure with a layer spacing $d = 39.6$ Å, the same as NOBOW. The extended molecular length of $L = 50$ Å indicates that the molecules are tilted, the **h**-**m** molecular plane [Fig. 2(a)] rotated relative to the layer normal **z** by the Euler angle $\theta_{\text{xray}} = \cos^{-1}(d/L) = 38°$. Bulk electro-optical measurements give $\theta_{\text{eo}} = 35°$ [10].

Freely suspended films with an integer number of smectic layers ($1 \leq N < 10$) were drawn in air. The in-plane azimuthal orientational textures of the high temperature smectic phase were imaged with depolarized reflected light microscopy (DRLM) [19], using obliquely incident $\lambda = 514$ nm Ar^+ laser light (angle of incidence = 7°) polarized normal to the plane of incidence to illuminate a

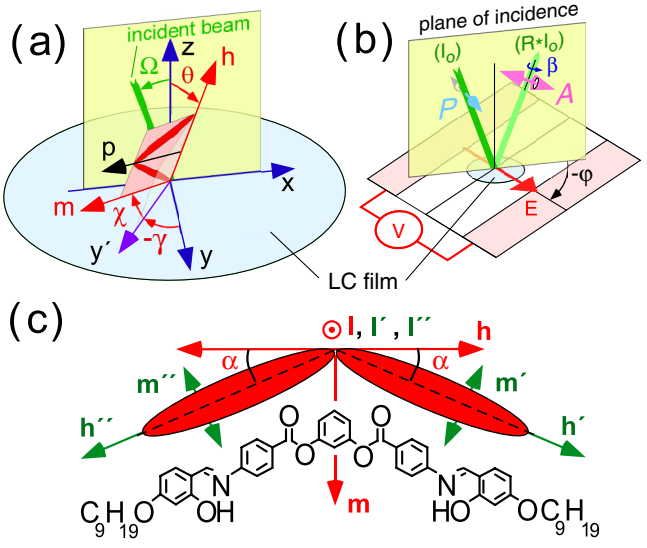

FIG. 2 (color online). (a) Model calculation geometry, illustrating the orientation of the molecular frame (**h**, **m**, ***l***) relative to the lab frame (**x**, **y**, **z**), and showing the SmC tilt θ, the SmCG χ rotation, and the overall azimuthal orientation γ. (b) Geometry of the DRLM experiment showing incident light polarized perpendicular to the plane of incidence, reflected light passing through an analyzer uncrossed by an angle β, and the stage rotation φ of the plane of incidence from the electric field direction. (c) The bent-core molecule NORABOW sketched in the **h**-**m**-***l*** molecular frame. The biaxial dielectric tensor is calculated by combining two uniaxial subfragments diagonal, respectively, in the $\mathbf{h}'$-$\mathbf{m}'$-$\boldsymbol{l}'$ and $\mathbf{h}''$-$\mathbf{m}''$-$\boldsymbol{l}''$ frames (**h**—high, **m**—medium, ***l***—low refractive index).

~300 μm diameter spot on the film. Film thickness was measured by laser reflectivity [9], and single-layer ($N = 1$) films selected for study. Observations of multilayer films and bulk phases are discussed elsewhere [20]. As is typical for smectics, the I-Sm transition was elevated in temperature in films a few layers thick, in this case ~30 °C higher than in the bulk. Electrodes [pink areas, Fig. 2(b)] enabled application of an in-plane electric field **E**. A crossed or slightly uncrossed analyzer showed an optic axis tilted relative to the layer normal, and revealed the brush patterns characteristic of smooth optic axis reorientation $\varphi(x, y)$ about **z**, typical of films of fluid, tilted smectics [19,21]. DRLM images of NORABOW were compared with those of NOBOW, which exhibits the SmCP layer structure in bulk and in thin films [4,7].

As expected from the B2-like behavior of the bulk, the response of single-layer films to in-plane electric fields revealed an in-plane polarization, evidenced by the stabilization of 2π walls of reorientation of φ [19]. By applying a 20 Hz ac field, it was possible to drive circular electrohydrodynamic flow of the film, which wound up the orientation field $\varphi(x, y)$, generating areas in which the lines of constant $\varphi(x, y)$ were nested rings [22] with $\varphi(x, y)$ varying monotonically with radius through many multiples of 2π. With the field removed, such ring structures, shown in Figs. 1 and 3, enabled the quantitative analysis of the φ dependence of the DRLM reflectivity $R_1(\beta, \varphi)$ (the ratio of the depolarized to polarized reflected intensity) as a function of β, the uncrossing angle of the analyzer [Fig. 2(b)]. $R_1(\beta, \varphi)$ was measured vs position through several rings of director reorientation (see Fig. 3 for typical paths), for a range of β values near crossing ($\beta \approx 0°$). The incident linearly polarized light [Fig. 2(b)] is resolved in the film into orthogonally polarized normal modes governed by the in-plane optical anisotropy associated with the projection of the biaxial dielectric tensor onto the film plane. These modes have slightly different reflection coefficients, so that the reflected light is linearly polarized but in general rotated through a small angle relative to the incident polarization in a way that depends on the in-plane principal axis orientation and anisotropy. Both the sign and magnitude of the rotation of the reflected polarization can be probed in detail by measuring the reflected intensity with the analyzer slightly decrossed. Typical ring patterns in NORABOW are shown in Fig. 3, along with corresponding plots of $R_1(\beta, \varphi)$ measured over 2π intervals in azimuthal orientation. The sensitivity to small changes in β is evident. When $E = 0$, the origin of the azimuth $\varphi(x, y)$, defined as **P** being parallel to **E**, is not known, so it is treated as a fitting parameter when comparing with the calculated reflectivity. Along a path normal to the rings, the director field forms alternating bands of 2D splay and bend deformation. The smooth variation of intensity in the rings indicates that the splay and bend elastic constants are nearly the same in NOBOW, as well as in NORABOW.

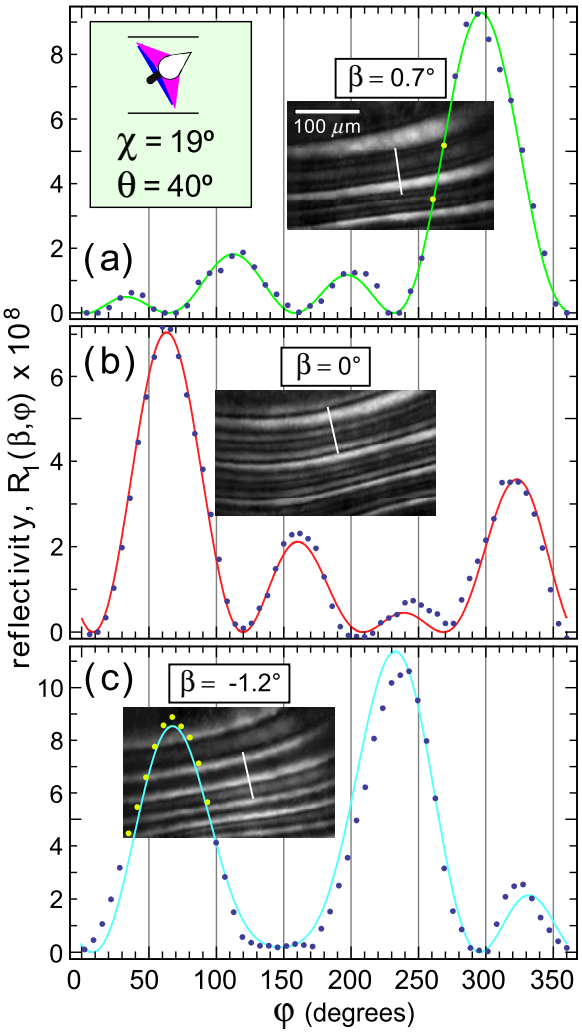

FIG. 3 (color online). Model and experimental DRLM reflectivity, $R_1(\theta, \beta, \varphi)$, of a one-layer thick NORABOW film at $T = 165\,^{\circ}\mathrm{C}$, for different analyzer uncrossing angles β. The experimental data are retrieved from paths such as those indicated by the white lines on the ring winding pattern images. Measurements (symbols) and the fitted model (curves) are shown for (a) $\beta = 0.7°$, (b) $\beta = 0°$, and (c) $\beta = -1.2°$. The inset in (a) shows a schematic drawing of the overall best-fit structure.

Theoretical reflectivity $R_1(\theta, \chi, \beta, \gamma)$ was calculated using the Berreman 4×4 matrix method [23], assuming each molecule to be made up of half-arms modeled by uniaxial rods connected at one end at an angle $\pi - 2\alpha$ [Fig. 2(c)]. Each layer of bent-core molecules then is taken to be two sublayers, each sublayer an array of uniformly tilted, unixial molecular half-arms [24,25]. The uniaxial sublayers are assigned the dielectric constants of DOBAMBC ($\varepsilon'_l = 2.2$, $\varepsilon'_m = 2.2$, $\varepsilon'_h = 2.9$), as these, when used for NOBOW, give the correct indices of refraction for its B2 phase [7]. The laboratory frame dielectric tensor of one bent-core molecular layer is obtained by starting with the optical uniaxes of the two sublayers along the layer normal (**h**, **m**, and ***l***, respectively, along **z**, **y**, and **x**, Fig. 2(a)] and rotating them about ***l*** by $\alpha = \pm 24°$ respectively [Fig. 2(c)], the angle obtained from Gaussian calculations of the three-ring core of NORABOW and NOBOW [26] and the extrapolated thickness of the core sublayer in NOBOW [26]. Then the rotations θ about **y**, χ about **h** [Fig. 2(a)], and ultimately the model azimuth γ about **z** [27], are systematically varied in order to obtain the $R(\theta, \chi, \beta, \gamma)$ curves in Fig. 3. The symmetry properties of the DRLM $R_1(\beta = 0, \varphi)$ profiles directly reveal the symmetry of the principal axis orientations. Thus, for the C_2 structure ($\chi = 0°$), $R_1(\theta, \chi = 0, \beta = 0, \varphi)$ must be reflection symmetric about $\varphi = 90°$ and 270°, and the lack of such symmetry is evidence for nonzero χ, as illustrated for the C_i case in Fig. 1. Specifically, the triclinic states, in which none of the principal axes lies in the film plane (C_i and C_1 in Fig. 1) have $R_1(\beta = 0, \varphi)$ profiles with unequal peaks.

Detailed comparison of the measured reflectivity was made with the $R_1(\theta, \chi, \beta, \gamma)$ curves obtained from the optical modeling. With γ the independent variable, θ fixed to within a few degrees by the layer spacing measurement, and the decrossing angle β selected and known in each experiment, only the single parameter χ controls the shape of $R_1(\theta, \chi, \beta, \gamma)$ and this can be determined unambiguously. Figure 3 shows ring textures with the polarizers crossed and slightly decrossed, along with intensity profile data averaged over several paths such as those indicated by the white lines. Best-fit values give $\theta = 40° \pm 1°$ and $\chi = 19 \pm 1°$.

The reflectivity of NOBOW films with $N \leq 4$ layers, on the other hand, exhibits no observable deviation from the symmetric pairs of large and small intensity peaks expected for the single SmCP layer shown in Fig. 1, or for $\mathrm{SmC_SP_A}$ multilayer films (the case $N = 2$ is shown in Fig. 4) in the absence of a SmCG χ rotation. Additionally, the optical phase shift and polarization rotation found in precision ellipsometric measurements are consistent with the SmCP (C_2) layer structure [7]. This is remarkable because for two-layer films, those that are $\mathrm{SmC_SP_A}$ must, by symmetry, be $\mathrm{SmC_SP_AG_A}$, and thus be triclinic (C_i) rather than monoclinic (C_2), as illustrated in Fig. 4. The C_i $\mathrm{SmC_SP_AG_A}$ state, with its opposing **z** polarizations in the two layers, is, in a two-layer $\mathrm{SmC_SP_A}$ film, an unavoidable consequence of the polar environment of each layer resulting from having a smectic layer on one side and air on the other. However, in NOBOW the rotation about χ is apparently so small that the deviation of $R(\beta = 0, \varphi)$ from the symmetric C_2 pattern has not been detectable, even in high-precision measurements [4,7]. In NOBOW, therefore, the χ rotation is quite small ($|\chi| < 2°$), even in the presence of a strong asymmetry driving χ (the surface polarization), whereas in NORABOW the χ rotation is large ($|\chi| \sim 20°$) and is adopted as a broken symmetry even in an $N = 1$ film, where there is no external asymmetry driving χ rotation. In 4-layer NORABOW

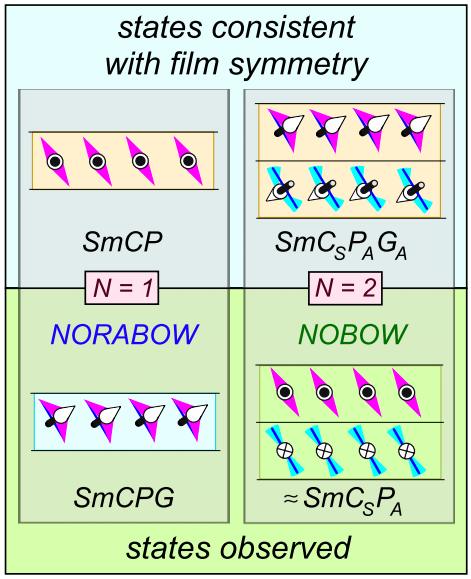

FIG. 4 (color online). Comparison of the structures of one-layer NORABOW films and two-layer NOBOW films, comparing the states consistent with the film symmetry with the states observed. In a single-layer film, NORABOW breaks symmetry to become triclinic, whereas in the triclinic environment of a two-layer film, NOBOW resists triclinic distortion, remaining nearly monoclinic.

films [20] both the internal and surface layers have θ and χ similar to those found here, an indication that, as in NOBOW, the layer environment only weakly perturbs the preferred internal layer structure. Bulk NORABOW exhibits phases of such layers in which the G ordering of adjacent layers is anticlinic, i.e., SmCPG$_A$, and which can be either of the same chirality or of alternating chirality [20].

In conclusion, study of the optical symmetry of the high temperature liquid crystal phase of NORABOW produces direct evidence for the least-symmetric fluid structure: a liquid smectic layer with internally stabilized chiral triclinic symmetry, generated by spontaneous adoption of in-plane polar ordering and an optical dielectric tensor with none of the principal axes oriented in or normal to the layer plane.

This work was supported by NASA Grant NAG-NNC04GA50G, NSF Grant 0606528 and by NSF Materials Research Science and Engineering Center Grant No. DMR 0820579.

[1] P. G. de Gennes, *The Physics of Liquid Crystals* (Oxford, London, 1975), p. 281.
[2] *International Tables for Crystallography* (Kluwer Academic, Dordrecht/Boston/London, 1983), Vol. A, Table 4.3.1.
[3] T. Niori, T. Sekine, J. Watanabe, T. Furukawa, and H. Takezoe, J. Mater. Chem. **6**, 1231 (1996).
[4] D. R. Link, G. Natale, R. Shao, J. E. Maclennan, N. A. Clark, E. Körblova, and D. M. Walba, Science **278**, 1924 (1997).
[5] R. B. Meyer, L. Liebert, L. Strzelecki, and P. Keller, J. Phys. (Paris), Lett. **36**, 69 (1975).
[6] C. Bahr and D. Fliegner, Phys. Rev. Lett. **70**, 1842 (1993).
[7] D. A. Olson, A. Cady, W. Weissflog, H. T. Nguyen, and C. C. Huang, Phys. Rev. E **64**, 051713 (2001).
[8] D. A. Olson *et al.*, Phys. Rev. E **63**, 041702 (2001).
[9] C. Y. Young, R. Pindak, N. A. Clark, and R. B. Meyer, Phys. Rev. Lett. **40**, 773 (1978).
[10] D. M. Walba, E. Körblova, R. Shao, and N. A. Clark, J. Mater. Chem. **11**, 2743 (2001).
[11] T. Akutagawa, Y. Matsunaga, and K. Yasuhara, Liq. Cryst. **17**, 659 (1994).
[12] A. Jákli, D. Krüerke, H. Sawade, and G. Heppke, Phys. Rev. Lett. **86**, 5715 (2001).
[13] A. Jákli, G. Nair, H. Sawade, and G. Heppke, Liq. Cryst. **30**, 265 (2003).
[14] A. Eremin, S. Diele, G. Pelzl, H. Nádasi, and W. Weissflog, Phys. Rev. E **67**, 021702 (2003).
[15] A. Jákli, D. Krüerke, and G. G. Nair, Phys. Rev. E **67**, 051702 (2003).
[16] J. P. Bedel, J. C. Rouillon, J. P. Marcerou, H. T. Nguyen, and M. F. Achard, Phys. Rev. E **69**, 061702 (2004).
[17] S. Rauch, P. Bault, H. Sawade, G. Heppke, G. G. Nair, and A. Jákli, Phys. Rev. E **66**, 021706 (2002).
[18] D. A. Coleman *et al.*, Science **301**, 1204 (2003).
[19] R. Pindak, C. Y. Young, R. B. Meyer, and N. A. Clark, Phys. Rev. Lett. **45**, 1193 (1980).
[20] N. Chattham, E. Körblova, R.-F. Shao, D. M. Walba, J. E. Maclennan, and N. A. Clark, Liq. Cryst. **36**, 1309 (2009).
[21] J. Z. Pang, C. D. Muzny, and N. A. Clark, Phys. Rev. Lett. **69**, 2783 (1992).
[22] D. R. Link, L. Radzihovsky, G. Natale, J. E. Maclennan, N. A. Clark, M. Walsh, S. S. Keast, and M. E. Neubert, Phys. Rev. Lett. **84**, 5772 (2000).
[23] D. W. Berreman, J. Opt. Soc. Am. **62**, 502 (1972).
[24] D. A. Olson, X. F. Han, P. M. Johnson, A. Cady, and C. C. Huang, Liq. Cryst. **29**, 1521 (2002).
[25] N. Chattham, Ph.D. thesis, Department of Physics, University of Colorado, Dissertation Abstracts #3136608.
[26] L. E. Hough *et al.*, Science **325**, 456 (2009).
[27] Only two Euler angles specify molecular orientation [Fig. 2(c)], because the azimuth γ is considered an independent variable in the analysis of the DRLM patterns. The palette of molecular orientations accessible following tilt θ of the molecular plane is the same whether the second rotation is "leaning" as in Ref. [12] or rotation about the bowstring, the choice made here.